Computer Models for Optimizing Interventions in Refractory Pulmonary Hypertension

Seong Woo Han

September 24, 2020

Abstract

This paper focuses on the simulation of computer models optimizing three surgical treatments of refractory pulmonary hypertension. The treatments are to create a condition normally considered as diseases, (1) atrial septal defect (ASD), (2) ventricular septal defect (VSD), or (3) patent ductus arteriosus (PDA), to generate a right-to-left shunt, allowing blood partially to bypass the lung and lower the pulmonary artery pressure. The models set up the methodology to examine the treatment results without actually operating the surgery to the patients. The models are based on the flexible circulation model and time-varying elastance model to show the hemodynamic changes and versatility of the valve in congenital heart disease. The models also compute the oxygen saturation of the circulation and examine the cross-sectional area of the connection we use in our model to describe the size of the defect. Numerical simulations are performed to compare the change of pressure and oxygen saturation in the pulmonary artery and systemic artery to study the impact of the treatments.

1 Introduction

Pulmonary hypertension is a type of high blood pressure when the pulmonary resistance elevates, affecting the arteries in our lungs and the right side of our heart. This makes deoxygenated blood flows over the body without getting oxygenated through the lungs. This paper focuses on refractory pulmonary hypertension in which such treatments do not respond to the disease. The clinical interest in this paper is surgical treatments, creating connections between chambers that do not normally exist in the circulation after birth, but that allow blood partially to bypass the lungs. The connections are creating a hole in the (1) atrial septum, (2) ventricular septum, or (3) connecting the main pulmonary artery with the aorta. Three proposed treatments create a condition that would normally be considered a disease state. That state, in case (1) is called atrial septal defect (ASD), in case (2) it is called ventricular septal defect (VSD), and in case (3) it is called patent ductus arteriosus (PDA). In all cases, the goal is to only create a right-to-left shunt to allow some blood to bypass the lung, which helps to lower the pulmonary artery pressure.

The understanding of the hemodynamic of ASD, VSD, and PDA is limited by the difficulty of measuring the shunt size. This paper describes mathematical models that help quantify the impact of these three surgical treatments. We demonstrate the connection between two chambers that we use in our model to describe the shunt size, or what we call the size of the defect. We also show oxygen saturation of the blood because modeling and computer simulation of oxygen in the blood can provide critical insight into the planning of cardiovascular surgeries. This simulation remains computationally challenging due to the complexity of hemodynamic in vascular networks, so we derive a general circulation model and time-varying elastance model that can be used to predict the patterns of blood flow and show the versatility of the valve model in congenital heart

disease. The approaches used in this paper can be adaptable to other heart defects with respect to characterizing pressure and oxygen saturation between chambers of the heart.

This paper provides the change of pressure and oxygen saturation inside the pulmonary artery and systemic artery varied by shunt size, simulating the result of three surgical treatments. To avoid the fluctuations in heartbeat, we only consider the mean value of the last ten cardiac cycles for the pressure and oxygen saturation. A comparison of pressure and oxygen saturation in each intervention is the main focus of our modeling, examining which surgical treatment has significant consequences in lowering pulmonary artery pressure. We show a schematic of the intervention setup for three treatments in Figure 1.

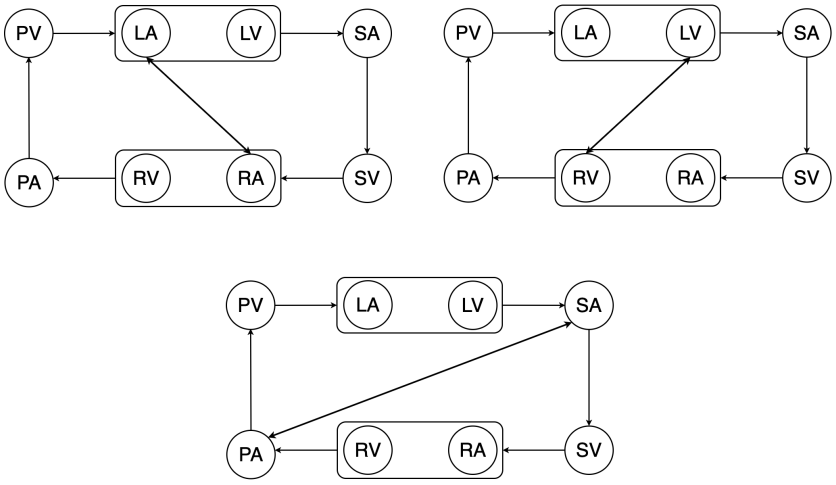

Figure 1: Specific model for the study of interventions in atrial septal defect (ASD), ventricular septal defect (VSD), and patent ductus arteriosus (PDA). Note that an arrow shows the flow direction considered positive, and the bidirectional arrows show the interventions. PA, pulmonary arteries; PV, pulmonary veins; LA, left atrium; LV, left ventricle; SA, systemic arteries; SV, systemic veins; RA, right atrium; RV, right ventricle.

2 Mathematical models descriptions

We assume a general model of the whole circulation [1]. The model circulation has the compliance relation for each N compliance chambers, numbered i = 1,2,...,N , where C_i is the compliance of chamber i, which may be constant for arteries and veins, but time-varying for chambers of the heart. The equation of a compliance chamber is its pressure-volume relation

$$V_i = (V_d)_i + C_i P_i, \quad i = 1, ..., N, \tag{1}$$

where V_i is the volume of compliance chamber i, P_i is the pressure in that chamber, and $(V_d)_i$ is the dead volume of chamber i, its volume when $P_i = 0$:

We also have the pressure-flow relationship for each of the resistance valve connected to the compliance chamber:

$$Q_{ij} = \frac{S_{ij}}{R_{ij}}(P_i - P_j) = S_{ij}G_{ij}(P_i - P_j), \quad i, j = 1, ..., N, \tag{2}$$

where

$$S_{ij} = \begin{cases} 1 & P_i > P_j, \\ 0 & P_i \leq P_j, \end{cases} \tag{3}$$

and where we characterize a resistance vessel by its conductance G, which is the reciprocal of the resistance, $G_{ij} = 1/R_{ij}$. We use conductance G instead of resistance R to cover the case when $R = \infty$. Both S_{ij} and S_{ji} cannot be 1 at the same time but can be zero at the same time only when $P_i = P_j$, in which there is no flow since there is no pressure difference.

We combine equations (1)-(3) to obtain

$$\begin{aligned} \frac{d}{dt}(C_i P_i) &= \sum_{j=1}^{N} (S_{ji} G_{ji}(P_j - P_i) - S_{ji} G_{ji}(P_i - P_j)) \\ &= \sum_{j=1}^{N} (S_{ij} G_{ij} + S_{ji} G_{ji})(P_j - P_i), \end{aligned} \tag{4}$$

Finally, using equation (1), we can express this as a N differential equations in the N unknowns $P_1, ..., P_N$:

$$\frac{C_i(t)P_i(t) - C_i(t - \Delta t)P_i(t - \Delta t)}{\Delta t} = \sum_{j=1}^{N} (S_{ij}(t)G_{ij} + S_{ji}(t)G_{ji})(P_j(t) - P_i(t)) \tag{5}$$

We put these equations in a standard form as following:

$$\sum_{j=1}^{N} A_{ij}(t)P_j(t) = C_i(t - \Delta t)P_i(t - \Delta t), \quad i = 1, ..., N, \tag{6}$$

where

$$A_{ij}(t) = -\Delta t(S_{ij}(t)G_{ij} + S_{ji}(t)G_{ji}), \quad i \neq j, \tag{7}$$

$$A_{ii}(t) = C_i(t) - \sum_{j:j \neq i} A_{ij}(t), \tag{8}$$

We provide the parameter values used for the model circulation in Table I. Compliance and dead volume parameters are the standard case for the normal adult circulation [3]. We set the R_p, Pulmonary resistance, 1.5 times bigger than the systemic resistance, $R_s = 17.5$ to make a disease state for our model.

2.1 Oxygen model

An important characteristic of congenital heart disease is that the normal pattern of oxygen saturation of the blood over the chambers is disrupted. The oxygen concentration is a very useful indicator for diagnosis and treatment [2]. In this subsection, we compute the oxygen model by the following differential equation:

$$\frac{d}{dt}([O_2]_i)V_i) = \sum_{\substack{j=1 \\ j \neq i}}^{N} ([O_2]_j Q_{ji} - [O_2]_i Q_{ij} + M_{ji}) \tag{9}$$

Parameters	Compliance (C)	Dead Volume (Vd)	Pressure (P)
Units	mmHg/(L/minutes)	L	mmHg
RVS	0.0003	-	-
LVS	0.0003	-	-
RVD	0.0146	-	-
LVD	0.0146	-	-
LV	-	0.010	5
RV	-	0.010	2
SA	0.00175	80	
PA	0.00175	100	
SV	1.75	0	4
PV	0.08	0	5

Table 1: Parameters for the heart model: RVS, minimum systolic value of right ventricle; LVS, minimum systolic value of left ventricle; RVD, maximum diastolic value of right ventricle; LVD, maximum diastolic value of left ventricle; LV, left ventricle; RV, right ventricle; SA, systemic artery; PA, pulmonary artery; SV, systemic vein; PV, pulmonary vein.

where $[O_2]_i$ is the oxygen concentration in chamber i, Q_{ji} is the blood from j to i, and M_{ji} is the rate of oxygen consumption by metabolism along the vessels from j to i. In this equation, we examine the change of oxygen concentration from chamber j into chamber i to see the difference in oxygen concentration when a certain rate of oxygen is consumed by the body (see Figure 2).

A numerical method for these equations is discretized with the backward Euler method:

$$\frac{([O_2]_i V_i)^{n+1} - ([O_2]_i V_i)^n}{\Delta t} = \sum_{\substack{j=1 \\ j \neq i}}^{N} ([O_2]_j Q_{ji} - [O_2]_i Q_{ij} + M_{ji}) \tag{10}$$

$$[O_2]_i^{n+1} V_i^{n+1} = [O_2]_i^n V_i^n + \Delta t \cdot \sum_{\substack{j=1 \\ j \neq i}}^{N} ([O_2]_j Q_{ji} - [O_2]_i Q_{ij} + M_{ji}) \tag{11}$$

By updating the total oxygen amount and dividing the amount by the volume of compliance chamber i, we derive the oxygen concentration in chamber i:

$$[O_2]_i^{n+1} = \frac{1}{V_i^{n+1}} \cdot \{[O_2]_i^n V_i^n + \Delta t \cdot \sum_{\substack{j=1 \\ j \neq i}}^{N} ([O_2]_j Q_{ji} - [O_2]_i Q_{ij} + M_{ji})\} \tag{12}$$

We assume the initial oxygen concentration as 10 mmol/L because the potential oxygen-carrying capacity of the blood in hemoglobin is 2.5 mmol/L, and each hemoglobin molecule carries four oxygen molecules. We also assume the metabolism consumption within the oxygen concentration. The normal blood flow rate of oxygen is 5.6 L/min and the mixed venous saturation that helps assess the tissue oxygen delivery is 65-75%, so the tissue oxygen extraction is 25-35%. This makes the rate of consumption by the body as 16.8 mmol/min.

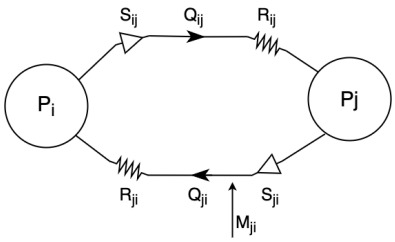

Figure 2: General model of the whole circulation. A pair of compliance chambers is each labeled as P_i and P_j. Every such pair in the model is connected by a pair of resistance vessels equipped with valve,R_{ij} ,pointing in opposite directions. $S_{ij} = 0$ or 1 denotes the state of the valve that allows from compliance chamber i into compliance change j. Q_{ij}, the flow from j to i. M_{ji}, the rate at which oxygen is carried from j into i by blood flowing into that chamber by metabolism.

2.2 Heart model

We now specify the time-varying elastance model for the left ventricle and right ventricle to demonstrate the versatility of the valve model[4]. Functional properties of each chamber are specified with maximal (E_{max}) and minimal (E_{min}) elastance that control systolic contractility and diastolic stiffness respectively. We set the value of E(T) and E(0) equal to set the periodic function exactly continuous:

$$E(t) = k(\frac{g_1}{1+g_1})(\frac{1}{1+g_2} - \frac{1}{1+g_{2T}}) + E_{min} \tag{13}$$

where

$$g_1 = (\frac{t}{\tau_1})^{m_1}, \quad g_2 = (\frac{t}{\tau_2})^{m_2}, \quad g_{2T} = (\frac{T}{\tau_2})^{m_2} \tag{14}$$

and k is a scaling factor that ensures max(E) = E_{max}, given by

$$k = \frac{E_{max} - E_{min}}{max[(\frac{g_1}{1+g_1})(\frac{1}{1+g_2} - \frac{1}{1+g_{2T}})]} \tag{15}$$

Parameter values used for the heart chambers are provided in Table II, with τ_1 controlling the timescale of contraction, τ_2 controlling the duration of systole, and m_1 and m_2 govern contraction and relaxation respectively. Chamber elastance parameters are chosen from the normal range for healthy adult humans [5-10] with τ and m estimated from previously employed values [11].

Parameters	Symbol	Units	Left Ventricle	Right Ventricle
Minimal elastance	E_{min}	mmHg/L	0.08*1000	0.08*1000
Maximal elastance	E_{max}	mmHg/L	30.00*1000	30.00*1000
Contraction rate constant	m_1	-	1.32	1.32
Relaxation rate constant	m_2	-	27.4	27.4
Systolic time constant	τ_1	min	0.269T	0.269T
Diastolic time constant	τ_2	min	0.452T	0.452T
Time constant	T	min	0.0125	0.0125

Table 2: Parameters for the heart model.

2.3 Shunt size model

To demonstrate the connection between two chambers, we introduce the Gorlin equation to examine the relationship between the cross-sectional area of the connection and the parameter that we use in our model to describe shunt size.

Consider two chambers, denoted by the indices 1 and 2, separated by a wall with a hole in it, and let A_0 be the cross-sectional area of the hole. We assume that the velocity of the fluid as it goes through the hole is much larger than the velocity in the two chambers that we consider the fluid in each of the two chambers as if it were at rest. Let Q be the volume of blood flow per unit time through the hole, with the direction from chamber 1 to chamber 2 considered positive.

$$v = Q/A_0. \tag{16}$$

An important complication is that the relationship between pressure and flow through a hole connecting two chambers is not linear. Let P_1 and P_2 be the pressures in the two chambers, and let P_0 be the pressure within the hole. Suppose, for example, that $Q > 0$. By Bernoulli's equation in the upstream chamber up to the hole itself,

$$\begin{aligned} P_0 &= P_1 - \frac{1}{2}\rho v^2 \\ &= P_1 - \frac{\rho}{2A_0^2}Q^2. \end{aligned} \tag{17}$$

In the region downstream of the hole, Bernoulli's equation does not apply because the flow there is dominated by turbulent eddies that dissipate energy. The result is that the pressure is relatively constant in the downstream region:

$$P_2 = P_0. \tag{18}$$

It follows that

$$P_1 - P_2 = \frac{\rho}{2A_0^2}Q^2, \quad Q > 0. \tag{19}$$

By the same reasoning, for flow in the other direction

$$P_2 - P_1 = \frac{\rho}{2A_0^2}Q^2, \quad Q < 0. \tag{20}$$

Equations (5) and (6) can be combined as follows:

$$P_1 - P_2 = \frac{\rho}{2A_0^2}|Q|Q, \tag{21}$$

and this shows that the hydraulic resistance of the hole is given by

$$R = \frac{\rho}{2A_0^2}|Q|, \tag{22}$$

Note that the above formula for R is independent of viscosity. In reality, there is a very small viscous resistance as well, so we modify the above formula to read

$$R = R_{visc} + \frac{\rho}{2A_0^2}|Q|, \tag{23}$$

In most situations R_{visc} is negligible, but we should include it to prevent R from being zero, which would otherwise happen in principle every time that Q changes sign. If R_{visc} is included only

for this reason, we choose with very small number of $R_{visc} = 0.1$ mmHg/(liter/min). Evaluating the conductance of the hole from equation (9), we get

$$G = \frac{1}{R_{visc} + \frac{\rho}{2A_0^2}|Q|} \tag{24}$$

In this equation, the value of $|Q|$ can be taken from the flow at the previous time step, and at the first time step, we can assume that $|Q| = 0$, so that we can start with $G = 1/R_{visc}$. In applying the foregoing, we use the length unit called the decimeter (dm) since we use the liter as our unit of volume, and this makes the area of the hole measured in units of dm^2. This is 1/100 of the area in cm^2. Also, since we measure pressure in mmHg, our unit of mass follows CGS units as below:

$$1mmHg = 0.1cmHg = \frac{(1.36g)(980cm/s^2)}{cm^2} = \frac{(1.36)(980)g}{cm\ s^2} \tag{25}$$

$$1g = \frac{1}{(1.36)(980)} mmHg\ cm\ s^2 \tag{26}$$

On the right-hand side of this equation, we multiply by 1 dm/10cm and $(1min/60s)^2$ to obtain

$$1g = \frac{1}{(1.36)(980)(10)(60)^2} mmHg\ dm\ min^2 \tag{27}$$

Then, since the density of blood is approximately $1000g/dm^3$, we have the result that

$$\rho = 1000\frac{1}{(1.36)(980)(10)(60)^2} \quad = 0.00002084167\frac{mmHg\ min^2}{dm^2} \tag{28}$$

After evaluating A_0 in dm^2 and ρ from equation (14), and after choosing a small constant value of R_{visc}, we can evaluate G for the hole at each time step by using equation (10), with Q given by the value of the flow through the hole that was found at the previous time step. The value of G that is found in this way can be written into the matrix of conductance and then the time step proceeds to solve for all the pressures, from which the flows including the flow through the hole can be determined.

3 Results and Analysis

In this section, we describe some results from numerical simulations of our models to examine the impact of each surgical treatment. We first investigate the changes in pressure and oxygen saturation in the systemic artery and pulmonary artery varied by the shunt sizes in each intervention. Second, we compare the direction of shunt flow mean and the volume of blood flow (L/min) in the shunt area to see whether the shunt direction is positive, right-to-left, which allows some blood to bypass the lung. In our simulation, the time step duration is chosen to be Δt $= 10^{-2}$ minutes and the total number of time steps as 1000, which implies 100 time steps per cardiac cycle and simulation of 1000 cardiac cycles, to study the results in a steady-state.

3.1 Comparing pressure and oxygen saturation

First, we compare the pressure and oxygen saturation for each intervention. Figure 3 shows the change of pressure varied by shunt area in the systemic artery and pulmonary artery for each intervention. Results for atrial septal defect (ASD) are on the left, results for connection in the ventricular septal defect (VSD) is on the right, and results for patent ductus arteriosus (PDA) is on the bottom. Unlike the drastic pressure change in VSD and PDA, the pressure in ASD barely changes, implying ASD is not an ideal setup for lowering the pulmonary artery pressure. We also remark that the inset figures show very small changes in each artery for the ASD. Among the three interventions, PDA significantly lowers the pulmonary artery pressure up to 30 mmHg, implying PDA is the ideal option among three treatments.

We further investigate the oxygen differences for each intervention in Figure 4-6. Results from ASD, VSD, and PDA are arranged from the left panel to the right. We depict the amount of oxygen delivery by multiplying the systemic flow and oxygen saturation and dividing the product result by 10 to observe the oxygen molecules delivered in each intervention in mmol per minute. VSD has certain shunt area, 0.3 - 0.4 cm^2, where surgeons should avoid since the amount of oxygen delivery decreases and increases again afterward. For every intervention, we can observe the oxygen saturation decreases as the shunt area increases.

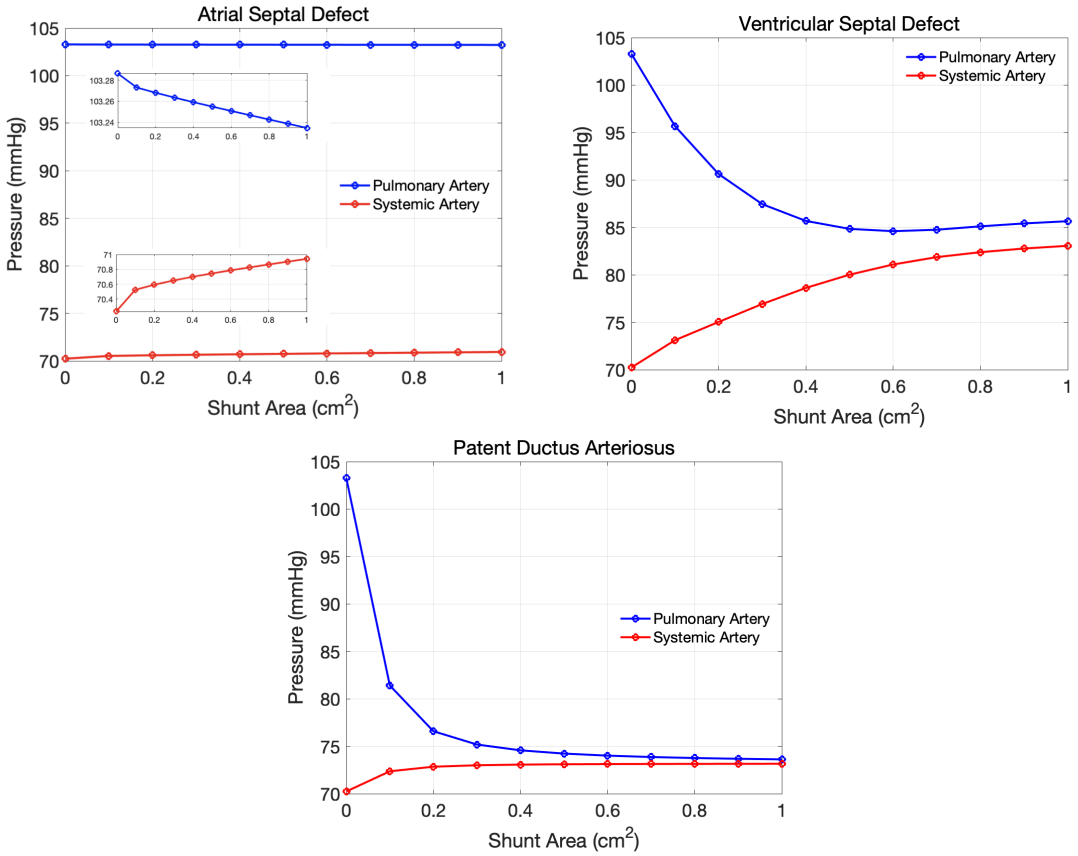

Figure 3: A comparison of pressure difference in pulmonary artery (blue) and systemic artery (red) varied by shunt area in ASD, VSD, and PDA. The inset figure shows a zoomed in portion of the results.

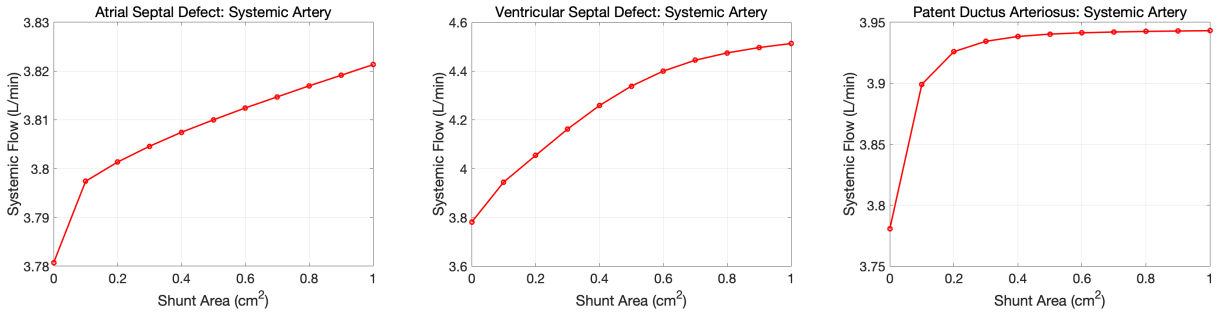

Figure 4: A comparison of volume of systemic flow in liters per minutes varied by shunt area. The left panel shows the results for ASD, the middle panel for VSD, and the right panel for PDA.

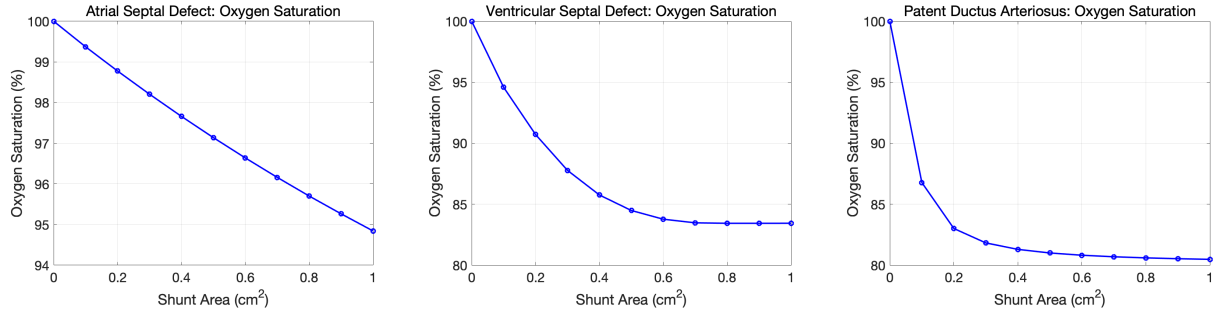

Figure 5: A comparison of oxygen saturation in percentage varied by shunt area. The left panel shows the results for ASD, the middle panel for VSD, and the right panel for PDA.

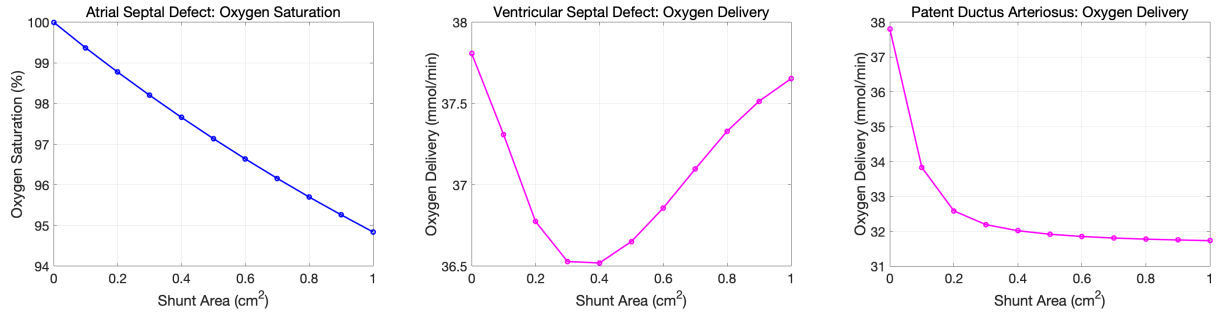

Figure 6: A comparison of oxygen delivery in mmol per minute varied by shunt area. The left panel shows the results for ASD, the middle panel for VSD, and the right panel for PDA.

3.2 Shunt direction and volume of blood flows in shunt area

In this subsection, we use our models to show the shunt direction of each intervention. We depict three directions of shunt flow mean, positive flow (right-to-left), negative flow (left-to-right), and overall flow (sum of positive and negative ones) for each intervention, to examine the impact of each treatment because our goal is to have the overall flow to be a right-to-left shunt to allow some blood pass the lung.

In Figure 7, we investigate that the shunt direction for ASD is bidirectional, implying the shunt flow reverses as the shunt area increases. The results for VSD and PDA show that the shunt direction is positive. We also include inset figures for both VSD and PDA to show the positive flow and overall flow correspond to each other, suggesting shunt direction for those interventions

is right-to-left. In Figure 8-10, we show the volume of blood flow in liters per minute to visualize the direction of blood flow. Results of the shunt areas in 0.1 cm^2 and 1 cm^2 are displayed for each intervention to examine the change of blood flow as the shunt area increases. We only consider the last ten cardiac cycles of blood flow to avoid fluctuations in heartbeat. As Figure 7 shows the shunt direction for ASD is bidirectional, Figure 8 also shows the blood flow alternating from positive to negative, implying the direction is bidirectional. Further, we can observe the blood flow increases as the shunt area increases for both VSD and PDA, implying the shunt direction is right-to-left.

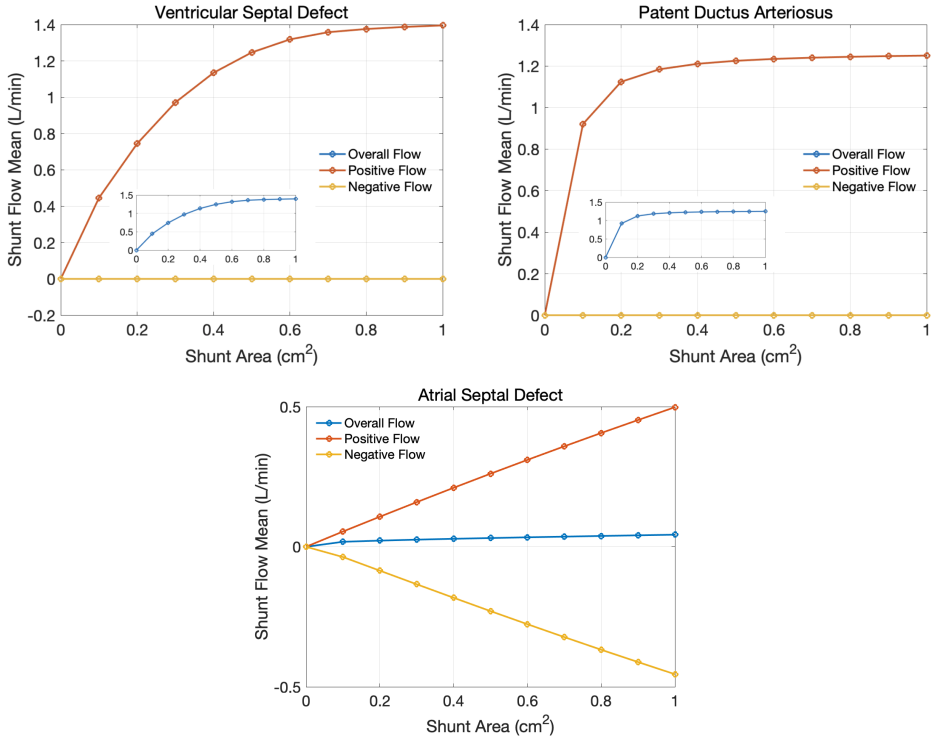

Figure 7: A comparison of shunt flow mean for ASD, VSD, and PDA: overall flow (blue), positive flow (orange), and negative flow (yellow). The inset figure shows a zoomed in portion of the results in VSD and PDA.

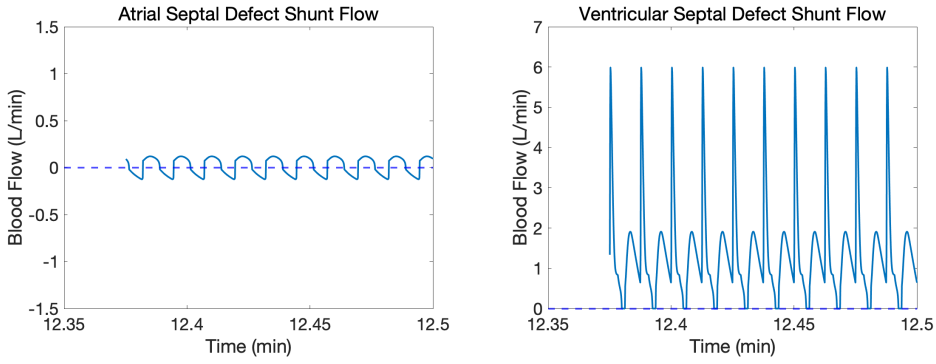

Figure 8: Results for blood flow change in ASD: the left panel shows the volume of blood flow when the shunt area is 0.1 cm^2. The right panel shows the volume of blood flow when the shunt area is 1 cm^2.

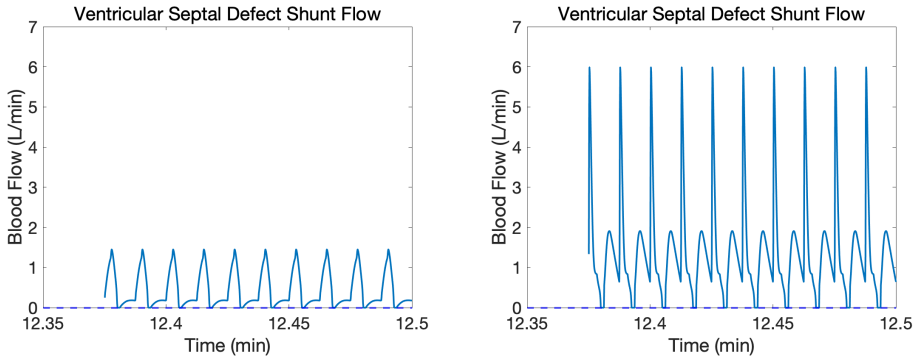

Figure 9: Results for blood flow change in VSD: the left panel shows the volume of blood flow when the shunt area is 0.1 cm^2. The right panel shows the volume of blood flow when the shunt area is 1 cm^2.

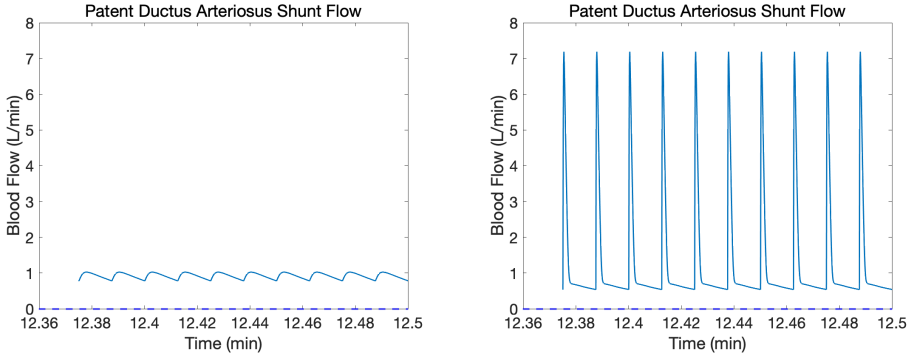

Figure 10: Results for blood flow change in PDA: the left panel shows the volume of blood flow when the shunt area is 0.1 cm^2. The right panel shows the volume of blood flow when the shunt area is 1 cm^2.

4 Conclusion

In this paper, we derived models to examine three surgical treatments results on refractory pulmonary hypertension without actually getting them performed to the patients. Two types of results were shown to see the impact of treatment effect: the change of pressure and oxygen saturation varied by the shunt area and visualization of the shunt direction and volume of blood flows in the shunt area. Among the three interventions, we investigate that creating atrial septal defect (ASD) gives the worst performance on reducing pulmonary artery pressure. Our models show that creating ventricular septal defect (VSD) and patent ductus arteriosus (PDA) only create a right-to-left shunt and PDA gives the best performance on reducing pulmonary artery pressure.

References

[1] Peskin, C.S. and Th, C.: Hemodynamics in congenital heart disease. Comput. Bioi. Med. 16:331-359, 1986.

[2] Tu, C. and Peskin, C.S.: Hemodynamics in transposition of the great arteries with compassion to ventricular septal defect. Comput. Bioi. Med. 19: 9.5-128, 1989.

[3] Hoppensteadt, Frank C., and Charles S. Peskin. Modeling and simulation in medicine and the life sciences. Vol. 10. Springer Science Business Media, 2012.

[4] Mynard, J. P., et al. "A simple, versatile valve model for use in lumped parameter and one-dimensional cardiovascular models." International Journal for Numerical Methods in Biomedical Engineering 28.6-7 (2012): 626-641.

[5] Kass DA, Midei M, Graves W, Brinker JA, Maughan WL. Use of a conductance (volume) catheter and transient inferior vena caval occlusion for rapid determination of pressure–volume relationships in man. Catheterization and Cardiovascular Diagnosis 1988; 15(3):192–202.

[6] Takeuchi M, Odake M, Takaoka H, Hayashi Y, Yokoyama M. Comparison between preload recruitable stroke work and the end-systolic pressure–volume relationship in man. European Heart Journal 1992; 13(Suppl E): 80–84.

[7] Senzaki H, Chen CH, Kass DA. Single-beat estimation of end-systolic pressure–volume relation in humans. A new method with the potential for noninvasive application. Circulation 1996; 94(10):2497–2506.

[8] Brown KA, Ditchey RV. Human right ventricular end-systolic pressure–volume relation defined by maximal elastance. Circulation 1988; 78(1):81–91.

[9] Dell'Italia LJ, Walsh RA. Application of a time varying elastance model to right ventricular performance in man. Cardiovascular Research 1988; 22(12):864–874.

[10] Maniar HS, Prasad SM, Gaynor SL, Chu CM, Steendijk P, Moon MR. Impact of pericardial restraint on right atrial mechanics during acute right ventricular pressure load. American Journal of Physiology - Heart and Circulatory Physiology 2003; 284(1):H350–H357.

[11] Stergiopulos N, Meister JJ, Westerhof N. Determinants of stroke volume and systolic and diastolic aortic pressure. American Journal of Physiology - Heart and Circulatory Physiology 1996; 270(6):H2050–H2059.